

Charge-carrier dynamics in hybrid plasmonic organic solar cells with Ag nanoparticles

Mei Xue,^{1,a)} Lu Li,² Bertrand J. Tremolet de Villers,³ Huajun Shen,¹ Jinfeng Zhu,¹ Zhibin Yu,² Adam Z. Stieg,^{4,5} Qibing Pei,² Benjamin J. Schwartz,^{3,4} and Kang L. Wang^{1,2}

¹Department of Electrical Engineering, Device Research Laboratory, University of California, Los Angeles, California 90095, USA

²Department of Material Science, University of California, Los Angeles, California 90095, USA

³Department of Chemistry and Biochemistry, University of California, Los Angeles, California 90095, USA

⁴California NanoSystems Institute, University of California, Los Angeles, California 90095, USA

⁵WPI Center for Materials Nanoarchitectonics (MANA), National Institute for Materials Science (NIMS), 1-1 Namiki, Tsukuba, Ibaraki 305-0044, Japan

(Received 4 April 2011; accepted 28 May 2011; published online 20 June 2011)

To understand the effects of Ag nanoparticles (NPs) on the performance of organic solar cells, we examined the properties of hybrid poly(3-hexylthiophene):[6,6]-phenyl-C₆₁-butyric-acid-methyl-ester:Ag NP solar cells using photoinduced charge extraction with a linearly increasing voltage. We find that the addition of Ag NPs into the active layer significantly enhances carrier mobility but decreases the total extracted carrier. Atomic force microscopy shows that the Ag NPs tend to phase segregate from the organic material at high concentrations. This suggests that the enhanced mobility results from carriers traversing Ag NP subnetworks, and that the reduced carrier density results from increased recombination from carriers trapped on the Ag particles. © 2011 American Institute of Physics. [doi:10.1063/1.3601742]

Bulk heterojunction (BHJ) photovoltaics based on interpenetrating networks of electron-donating conjugated polymers and electron-accepting fullerenes continue to be the focus of substantial interest as a potentially inexpensive route to harvest solar energy.^{1,2} Because organic materials suffer from low carrier mobilities, the active layers in BHJ devices tend to be quite thin (~100 nm), which in turn can result in poor light absorption. As a result, conjugated polymer-based solar cells continue to have significantly lower efficiencies than their inorganic counterparts with the current record hovering around 8%.³

To overcome the weak absorbance of the thin photoactive layers in BHJ solar cells, different approaches have been tried, such as using periodic nanostructures to trap light in the thin active layers^{4–6} incorporating metal nanoparticles (NPs) that can provide plasmonic enhancement.^{7–10} Although there have been a number of demonstrations of plasmon-enhanced absorption and charge generation in organic solar cells, to date none have resulted in devices with high efficiencies.^{8,9} This suggests that although the introduction of metal NPs enhances absorption, it also alters the operation of organic solar cells in ways that are detrimental to device performance.

In this letter, we use the photoinduced charge extraction with a linearly increasing voltage (photo-CELIV) technique¹¹ to elucidate the performance-limiting factors associated with the introduction of metal NPs to conjugated polymer/fullerene BHJ solar cells. We loaded organic solar cells fabricated from regioregular poly(3-hexylthiophene) (P3HT) and [6,6]-phenyl-C₆₁-butyric-acid-methyl-ester (PCBM) with Ag metal NPs at different concentrations. Our experiments show that despite the efficiency decrease upon the addition of Ag NPs, the carrier mobility in P3HT:PCBM

BHJ devices increases with increasing concentration of the Ag NPs. We find that the efficiency loss results from a significant decrease in the extracted carrier density upon the introduction of Ag NPs. Atomic force microscopy (AFM) experiments show that at high loadings, the Ag NPs phase segregate from the photoactive organic material. This suggests that carriers leave the organic phase to move on an aggregated subnetwork of Ag NPs, explaining the mobility increase. The decreased carrier extraction results from the fact that Ag NPs that are not physically contiguous act as carrier traps, leading to significantly enhanced recombination and thus lower overall net efficiency.

We fabricated our plasmonic hybrid organic solar cells with an active layer consisting of a ~250 nm thick BHJ film with P3HT:Ag NP weight ratios of 32:1, 16:1, 8:1, and 4:1. Additional details of our device fabrication are described in Ref. 12. The inset to Fig. 1 shows a schematic of our sandwich-structure hybrid plasmonic BHJ organic solar

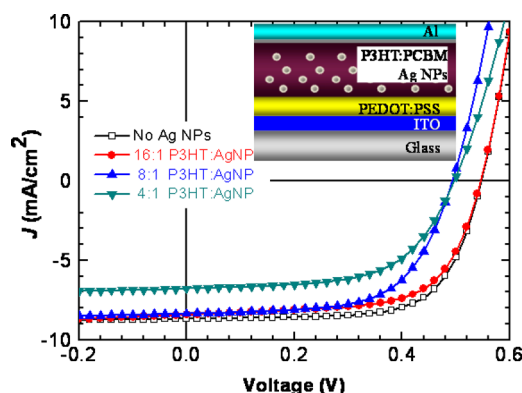


FIG. 1. (Color online) J-V characteristics of the hybrid plasmonic 1:1 P3HT:PCBM BHJ solar cells incorporated with Ag NPs at different concentrations. The control cell has the same device architecture but without Ag NPs in the active layer. The inset shows a schematic structure of our hybrid plasmonic BHJ solar cells.

^{a)}Electronic mail: mxue@ee.ucla.edu. Tel: +1-310-206-0207. FAX: +1-310-206-8495.

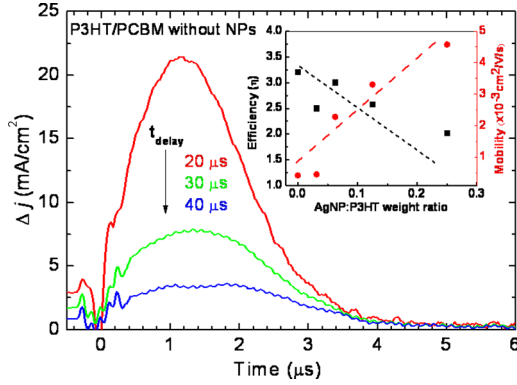


FIG. 2. (Color online) Photo-CELIV current transients, $j-j(0)$, collected at different values of t_{delay} for a P3HT:PCBM BHJ solar cell without Ag NPs. The inset shows the solar cell device efficiency and the charge-carrier mobility calculated using Eq. (1) for hybrid cells with different concentrations of Ag NPs. The mobility strongly increases with increasing concentration of Ag NPs.

cells; all of the data shown below represent the average behavior of at least five devices.

After preparing our solar cells, we used UV-visible absorption spectroscopy to confirm that the localized surface plasmon resonance of the added Ag NPs provided a significant absorption enhancement from 350–650 nm, as described in Ref. 12. We also verified that the addition of Ag NPs did not change the amount of fluorescence emitted both from films of pure P3HT and from P3HT:PCBM BHJ blends, confirming that the silver particles do not act as exciton dissociation sites.¹² This means that other than the enhanced absorption cross-section, Ag NPs do not affect the initial exciton creation or dissociation events in P3HT:PCBM solar cells.

Figure 1 shows the photovoltaic behavior of our hybrid plasmonic solar cells under AM1.5G illumination at 100 mW/cm². Our control P3HT:PCBM cells with no Ag NPs have a power conversion efficiency of 3.4% but the addition of Ag NPs at a 1:16 Ag:P3HT weight ratio lowers the device efficiency to 3.3%. Adding higher fractions of Ag NPs leads to even greater drops in efficiency, as illustrated by the black points in the inset of Fig. 2.

To understand the reasons for the drop in power conversion efficiency upon the addition of Ag NPs, we characterized the carrier mobility and recombination dynamics in these devices using photo-CELIV.¹¹ The details of our photo-CELIV experimental setup have been described elsewhere.¹³ Briefly, in photo-CELIV a short light pulse is used to create carriers in a device, which are then extracted by a linear voltage ramp that is applied after a time delay, t_{delay} . The time it takes the extracted current to reach its maximum value from the start of the voltage ramp, t_{max} , is related to the carrier mobility by¹⁴

$$\mu = \frac{2d^2}{3At_{\text{max}}^2 \left[1 + 0.36 \frac{\Delta j}{j(0)} \right]}, \quad (1)$$

where d is the thickness of the active layer, A is the slope of the voltage ramp, $j(0)$ is the capacitive current, and Δj is the extracted photocurrent transient. The integral of the current transient gives the total extracted carrier density, and the behavior of this integral as a function of t_{delay} can thus be used to track the carrier recombination dynamics.¹⁵

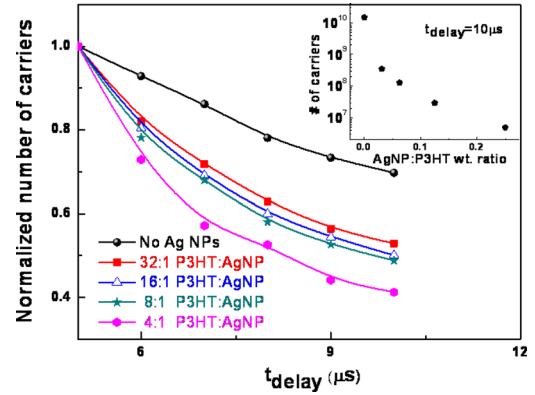


FIG. 3. (Color online) Dependence of the total extracted number of carriers in photo-CELIV experiments on t_{delay} for P3HT:PCBM BHJ solar cells with different concentrations of Ag NPs. The solid curves are fits to the carrier decays with a power law, $t^{-\alpha}$, with α equal to 1.4, 1.68, 1.72, 1.75, and 1.98, respectively, with increasing Ag concentration. The inset shows the total number of extracted carriers from BHJ solar cells with different concentrations of Ag NPs for $t_{\text{delay}}=10 \mu\text{s}$.

Figure 2 shows representative photo-CELIV current transients for one of our P3HT:PCBM control solar cells without Ag NPs for several values of t_{delay} . The data show that t_{max} remains essentially constant with t_{delay} and that the total amount of extracted charge decreases significantly as the t_{delay} increases. We used Eq. (1) and data such as that in Fig. 2 to calculate the carrier mobility in solar cells with a range of Ag NP concentrations; the results are shown as the red points in the inset to Fig. 2. Surprisingly, the carrier mobility increases dramatically with increasing concentration of the Ag NPs; at the largest concentrations, the mobility is increased by nearly an order of magnitude relative to control BHJ devices without Ag. The fact that the carrier mobility increase is roughly proportional to the NP concentration indicates that the NPs play a direct role in carrier conduction, likely by a hopping mechanism. If each Ag NP acts as a hopping site, the average hopping distance becomes smaller as the NP density in the active layer increases, explaining the observed increase in mobility.

Given that both light absorption¹² and carrier mobility increase with the addition of Ag NPs, why is adding NPs detrimental to the overall device performance? To investigate this, we integrated the transient current in our photo-CELIV experiments to determine the total amount of charge extracted from our devices, Q_e , for different values of t_{delay} ;

$$Q_e = S \int_0^{t_{\text{pulse}}} \Delta j dt, \quad (2)$$

where S is the cathode area. Figure 3 shows how the total amount of extracted charge changes as a function of both t_{delay} and Ag NP concentration. The number of extracted charges clearly decreases as a function of delay time, with the decrease roughly following a power law, $t^{-\alpha}$, with α increasing from ~ 1.4 to ~ 2.0 with increasing Ag concentration. The increase in α with increased Ag NP concentration is indicative of increased recombination losses due to localized (trapped) carriers,¹⁵ which presumably reside on the Ag NPs. Perhaps more strikingly, the inset of Fig. 3 also shows that the total number of the extracted carriers is reduced by several orders of magnitude as the amount of Ag NPs increases from 32:1 to 4:1 P3HT:Ag. Since the device power conversion efficiency is proportional to both the number of ex-

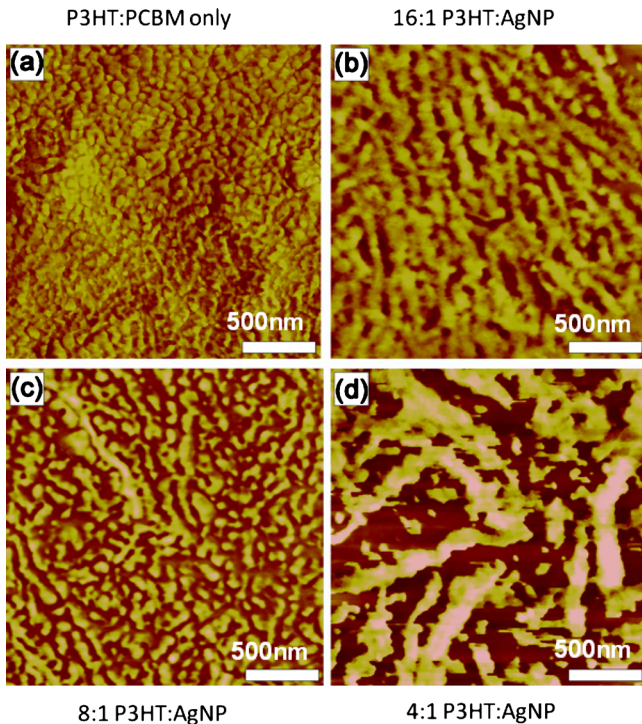


FIG. 4. (Color online) Representative AFM phase images of the surface of the active layer of P3HT:PCBM BHJ solar cells (a) without Ag NPs, (b) with 16:1 P3HT:AgNPs, (c) with 8:1 P3HT:AgNPs, and (d) with 4:1 P3HT:AgNPs, respectively.

tracted carriers and their mobility, the substantial decrease in the number of extracted carriers overwhelms the smaller mobility increase, resulting in the net lower device efficiency.

To understand why the addition of Ag NPs leads to opposing changes in carrier mobility and extracted carrier density, in Fig. 4 we show AFM phase images of the active layers of some of our BHJ solar cells with varying concentrations of Ag NP. The images show clearly that as the concentration of Ag NPs is increased from 16:1 to 4:1 P3HT:Ag, there is significant phase separation of the Ag NPs from the P3HT:PCBM BHJ organic material. Since the dodecyl side chains on the Ag NPs poorly dissolve in highly aromatic molecules such as P3HT and PCBM, the phase-segregated Ag NPs form their own subnetwork, with both the extent of the network and its degree of interconnectivity increasing with increasing loading of the NPs. This observation is consistent with the photo-CELIV measurements that show an increase in carrier mobility with increasing Ag NP concentration, suggesting that carriers can move along the Ag NP subnetwork.

The formation of a Ag NP subnetwork can also explain the reduced number of charges extracted from the device. Carriers trapped on the NP subnetwork likely have a difficult time hopping back onto the organic phase, leading to trapping that significantly enhances recombination, as suggested by the power-law recombination decays. With increasing Ag concentration, the recombination power law decay coefficient approaches 2, indicating that bimolecular recombination becomes the dominant recombination mechanism.¹⁶ This is consistent with our observation of increased mobility of the charge carriers on the Ag subnetwork—more mobile charges are more likely to find another charge carrier with which to recombine. Furthermore, the fact that Ag NPs provide trap-assisted recombination of the charge carriers might

also explain the reduced open-circuit voltage in the devices with high Ag NP concentrations.¹⁷

In summary, we have investigated the way in which the addition of Ag NPs alters the performance of plasmonic hybrid organic solar cells. Not only does the addition of Ag NPs enhance the local absorption, but it also leads to increased carrier mobility, since Ag particles are more conductive than organic materials such as P3HT and PCBM. The fact that carriers move on a subnetwork of Ag NPs, however, makes it difficult to extract them before they undergo recombination since dead-ends in the Ag NP network act as traps, leading to monomolecular recombination. At this stage, we are unable to determine whether it is the electrons or holes (or both) that travel on the Ag NP subnetwork because the photo-CELIV technique cannot distinguish the sign of the extracted charge(s). If both carriers move along the Ag NP subnetwork, then it would be difficult to avoid carrier loss due to enhanced recombination. If only one carrier moved along the metal, however, then it might be possible to intentionally create a NP subnetwork that could enhance both the mobility and extraction of the limiting carrier. Otherwise, to take advantage of plasmonically enhanced polymer-based BHJ solar cells, one needs to find a way to prevent the carriers from localizing on the metal NPs so that the NPs would serve only to enhance absorption and not to alter the motion of carriers through the device.

The authors thank the partial support of the KACST under the KACST-CAL Green Technology Center and the Nano and Pico Characterization Laboratory at the California NanoSystems Institute. B.J.S. acknowledges the support of funding through a DOE EFRC center under Contract No. DE-SC0001342:001.

¹G. Yu, J. Gao, J. C. Hummelen, F. Wudl, and A. J. Heeger, *Science* **270**, 1789 (1995).

²C. J. Brabec, N. S. Sariciftci, and J. C. Hummelen, *Adv. Funct. Mater.* **11**, 15 (2001).

³Y. Liang, X. Zheng, J. Xia, S. Tsai, Y. Wu, G. Li, C. Ray, and L. Yu, *Adv. Mater. (Weinheim, Ger.)* **22**, E135 (2010).

⁴M. Niggemann, M. Glatthaar, P. Lewer, C. Müller, J. Wagner, and A. Gombert, *Thin Solid Films* **511–512**, 628 (2006).

⁵G. Mariani, R. B. Laghumavarapu, B. Tremolet de Villers, J. Shapiro, P. Senanayake, A. Lin, B. J. Schwartz, and D. L. Huffaker, *Appl. Phys. Lett.* **97**, 013107 (2010).

⁶K. S. Nalwa, J. Park, K. Ho, and S. Chaudhary, *Adv. Mater. (Weinheim, Ger.)* **23**, 112 (2011).

⁷B. P. Rand, P. Peumans, and S. R. Forrest, *J. Appl. Phys.* **96**, 7519 (2004).

⁸A. J. Morfa, K. L. Rowlen, T. H. Reilly, M. J. Romero, and J. V. De, *Appl. Phys. Lett.* **92**, 013504 (2008).

⁹S. Kim, S. Na, J. Jo, D. Kim, and Y. Nah, *Appl. Phys. Lett.* **93**, 073307 (2008).

¹⁰H. A. Atwater and A. Polman, *Nature Mater.* **9**, 205 (2010).

¹¹G. Juška, K. Arlauskas, M. Viliūnas, K. Genevičius, R. Österbacka, and H. Stubb, *Phys. Rev. B* **62**, R16235 (2000).

¹²See supplementary material at <http://dx.doi.org/10.1063/1.3601742> for the details of device fabrication and for the UV-Visible light absorption and steady-state photoluminescence emission spectra of P3HT:Ag NP composite films with various P3HT:Ag NP weight ratios.

¹³B. Tremolet de Villers, C. J. Tassone, S. H. Tolbert, and B. J. Schwartz, *J. Phys. Chem. C* **113**, 18978 (2009).

¹⁴A. J. Mozer, G. Dennler, N. S. Sariciftci, M. Westerling, A. Pivrikas, R. Österbacka, and G. Juska, *Phys. Rev. B* **72**, 035217 (2005).

¹⁵A. J. Mozer, N. S. Sariciftci, L. Lutsen, D. Vanderzande, R. Österbacka, M. Westerling, and G. Juska, *Appl. Phys. Lett.* **86**, 112104 (2005).

¹⁶A. F. Nogueira, I. Montanari, J. Nelson, J. R. Durrant, C. Winder, N. S. Sariciftci, and C. Brabec, *J. Phys. Chem. B* **107**, 1567 (2003).

¹⁷M. Mandoc, W. Veurman, L. Koster, B. deBoer, and P. Blom, *Adv. Funct. Mater.* **17**, 2167 (2007).